Effect of Operating Conditions and Particle Properties on Performance of Vertical Air-Lift

Jana Chladek[1], *Gisle G. Enstad*[1,2], *and Morten C. Melaaen*[2]

[1] Department of POSTEC, Tel-Tek, Kjoelnes Ring 30, N-3918 Porsgrunn, Norway

[2] Department of Process, Energy and Environmental Technology, Telemark University College, Kjoelnes Ring 56, P.O. Box 203, N-3901 Porsgrunn, Norway

AUTHOR EMAIL ADDRESS:

jana.chladek@tel-tek.no; gisle.enstad@hit.no; morten.c.melaaen@hit.no

---

*CORRESPONDING AUTHOR: Tel: +47 35 57 41 45; Email: jana.chladek@tel-tek.no

ABSTRACT

The effect of the fluidization air flow rate and the transport air velocity on the solids mass flow rate and the pressure drop along the transport pipe was investigated in a vertical air-lift. The use of two different materials, glass (150 μm) and zirconium oxide (260 μm) particles (Geldart's B class), enabled to estimate the effect of particle properties on the air-lift performance. Different levels of the solids mass flow rate were obtained by varying the fluidization air flow rate while keeping the transport air velocity constant. The solids loading ratio varied between 2 and 16 for both types of particles. The pressure drop was nonlinearly related to the solids mass flow rate at most of the transport air velocities tested. State diagrams presenting the relationship between the transport air velocity, the solids mass flow rate, and the pipeline pressure drop were constructed to characterize the flow pattern and to compare the behavior of the glass and zirconium oxide particles. Owing to the larger size and higher density, the zirconium oxide particles displayed higher pressure drop values than the glass beads and the minimum pressure drop shifted towards higher transport air velocities. The velocity at the transition between dilute and dense phase conveying was approximately in the range of 7 to 10 m/s for glass beads and 10 to 12 m/s for zirconium oxide, at the solids mass flow rates tested. The flow patterns could be also effectively characterized from the analysis of the pressure drop fluctuations at different transport air velocities.

KEYWORDS

Pneumatic conveying; Vertical air-lift; Fluidization; Transport air velocity; Solids mass flow rate; Pipeline pressure drop; Pressure drop fluctuations

1. Introduction

Pneumatic conveying systems represent one of the principal means of transporting bulk powder and granular materials, both horizontally and vertically, in a variety of industries (e.g., mining, metallurgy, chemical, agriculture, food). The main advantages of pneumatic transport include elimination of material spillage and dust pollution, reduced fire and explosion hazards, flexibility in pipeline routing, alterations and potential expansion of pipeline capacity, low maintenance, reliability, ease of operation, and low manpower requirements. Some limitations are high power costs compared to other conveying systems (e.g., mechanical), attrition and degradation of friable materials, and difficulty to develop universal design and optimization procedures for pneumatic conveying of distinct materials [1-4].

Vertical air-lift is a special type of a pneumatic conveyor used for continuous vertical transport of solids into elevated silos or receivers. The system consists of a feed tank with two air supplies (fluidization and transport), vertical transport pipe, and a receiving tank. The powder material in the feed tank is fluidized to enhance the flowability of the air-solid mixture in the feeding zone. The transport air enters the bottom of the feed tank through a nozzle located below the inlet of the vertical transport pipe. The high velocity air stream entrains the solids and conveys them through the transport pipe into the receiving tank. In industrial applications, vertical air-lifts are typically operated in a continuous mode, with solids being continuously fed into the feed tank to maintain the hydrostatic pressure of the fluidized bed. The higher the hydrostatic pressure, the higher the solids entrainment into the transport pipe and consequently, the higher the conveying capacity [1]. Despite its use in aluminium and cement industry over the past decades, a general method for the system optimization has never been documented. Operating conditions leading to satisfactory performance are found in practice by the process of trial and error and/or practical experience. The lack of system optimization may substantially increase the operation costs without actually reaching the top performance.

Only a few publications have looked into the factors influencing the pneumatic transport of powder materials in a vertical air-lift or similar devices. Earlier studies [5, 6] on vertical pneumatic conveyor with a fluidized bed solids feeder showed that the solids mass flow rate was dependent on a combination of transport air flow rate, fluidization air flow rate, height of the fluidized bed, and length and diameter of the transport pipe. Recent work mainly focused on measuring particle velocity profiles in pipe cross-section using laser Doppler anemometry [7] and particle image velocimetry [8]. As expected, the particle velocity was shown to increase with increasing superficial air velocity and decreasing particle size and density [8]. Mathiesen and Solberg [7] also investigated the influence of distance z between the nozzle outlet and the transport pipe inlet on the solids mass flow rate and found that for a given transport air flow rate, the solids mass flow rate increased with increasing distance z. Similar behavior

was observed by Garic *et al.* [9] in a vertical pneumatic conveyor equipped with a spouted bed feeding device.

The flow behavior in pneumatic transport is generally described in the form of state diagrams where the pressure drop is plotted as a function of transport air velocity for different solids mass flow rates. Upon reducing the transport air velocity at constant solids mass flow rate, the solids concentration in the pipeline increases but the pressure drop decreases as a result of reduced wall friction. The flow regime is usually characterized as dilute or suspended flow until the pressure drop reaches a minimum where the transition from dilute to dense phase occurs. Further reduction in transport air velocity results in a non-uniform distribution of solids over the pipe cross-section and eventually pipeline blockage accompanied with a sharp pressure drop increase. The transport air velocity at the minimum pressure drop represents the minimum velocity to support a stable dilute gas-solid flow. To avoid unstable conditions encountered in dense phase and unnecessarily high pressure drops in dilute phase, vertical pneumatic conveying is mostly carried out in dilute phase near the point of the minimum pressure drop [1, 10].

The position of the minimum pressure drop on the state diagram is dependent on the particle properties, as well as the system characteristics and operating conditions. Because of the many factors involved, prediction of the minimum point is extremely difficult and additional experimental research is still needed for better understanding of the pneumatic conveying phenomena and successful modeling. No study on vertical air-lifts attempted yet to characterize the relationship between the transport air velocity, the solids mass flow rate, and the pressure drop in the form of state diagrams, nevertheless, this method proves the most useful in developing a successful pneumatic conveying system design.

The flow behavior characterized by the state diagrams and the effect of particle properties on the pressure drop profiles was extensively studied in other pneumatic conveying systems. Narimatsu *et al.* [11] studied the effect of particle diameter (1.00–3.68 mm) and density (935–2500 kg/m^3) on the dynamic fluid behavior during vertical pneumatic conveying of Geldart's D particles (spoutable). The pressure drop increased with increasing particle size and density in the dense phase regime while no significant changes in pressure drop were observed in the dilute phase regime. The position of the minimum pressure drop shifted to higher gas velocities as the particle size and density increased, which was attributed to greater slip force required for the transport of larger and heavier particles. Wang *et al.* [12] compared the flow characteristics of 20 μm (cohesive Geldart's C powders) and 66 μm (aeratable Geldart's A powders) glass beads in vertical pneumatic transport. As expected, the minimum pressure drop was higher for the larger diameter glass beads. However, the minimum pressure drop velocity was significantly higher for the 20 μm glass beads (11 m/s) than for the 66 μm glass beads (6.5 m/s). Wang *et al.* explained this behavior by the cohesive nature of the 20 μm glass beads, resulting in particle adhesion on the pipe wall and consequently, reduced solids friction. Addition of anti-static particles

revealed that the pressure gradients were also affected by electrostatic charging. Using glass beads of different diameters (35, 203, 340, and 580 μm) in horizontal pneumatic conveying, Herbreteau *et al.* [13] demonstrated that the minimum pressure drop (and the velocity at the minimum pressure drop) decreased with decreasing particle size, reached a minimum at a particle diameter of about 200 μm, and then increased. Comparison of the flow behavior of glass beads with cement and polystyrene beads revealed that the pressure drop profile was also dependent on particle shape and density. Hyder *et al.* [14] investigated the effect of particle size on pressure drop along straight horizontal pipeline in dilute phase pneumatic conveying using different materials with average particle diameter ranging between 30 and 3000 μm. Under identical conveying conditions, the pressure drop increased with increasing particle size, which was associated with additional energy needed to convey larger particles.

The objective of this study was to systematically investigate the effect of the transport air velocity and the fluidization air flow rate on the solids mass flow rate as well as the pipeline pressure drop in vertical air-lift. Glass and zirconium oxide particles with an average particle diameter of 150 and 260 μm, respectively, were used to estimate the effect of particle properties on the air-lift performance. State diagrams illustrating the relationship between the transport air velocity, the solids mass flow rate, and the pressure drop were constructed to identify the conditions for the transition between dilute and dense phase conveying. Attention was also drawn to the pressure drop fluctuations under different conveying conditions.

2. Experimental

2.1. Experimental apparatus

Experiments were conducted in a 4 m high vertical air-lift (Figure 1). The flow rate of the fluidization and the transport air was measured by a flow meter *(1)*. The fluidization air was supplied at several positions to the cone of the feed tank *(2)* and distributed over an air distribution plate *(3)* (air permeable fabric) to achieve uniform fluidization of the solids column. The transport air entered the feed tank through a cylindrical steel nozzle *(4)* with an internal diameter (ID) of 15 mm. The nozzle outlet could be positioned at a variable distance below the transport pipe inlet, however, in this study, the distance was fixed at 3 cm (i.e., z = 3 cm). The transport pipe *(5)* was made of steel and had ID of 42 mm. The conveying air carried the solids through the transport pipe into the receiving tank *(6)*, which was vented to atmosphere. A paper bag filter *(7)* at the air exhaust was used to collect any escaping particles. Glass windows *(8)* were installed on the feed and the receiving tank for easy inspection. The feed and the receiving tank were connected with a bleed line *(9)* (ID = 80 mm) to avoid any pressure build-up between the tanks. The pressure difference between the feed and the receiving tank was monitored with a differential pressure transmitter *(10)* (0–100 mbar, EJX110A, Yokogawa) and was less than 0.4 mbar

for all experiments. The pressure drop along the transport pipe was measured by another differential pressure transmitter *(10)* (0–100 mbar, EJX110A, Yokogawa) that was connected to two pressure taps positioned approximately 1.15 and 2.25 m above the inlet of the transport pipe. It was shown previously based on the particle velocity profiles that within this region, the flow was fully developed [7]. Three load cells *(11)* (Z6FC3, HBM) were mounted on the receiving tank to evaluate the solids mass flow rate during the transport. The differential pressure transmitters and the load cells were connected to a data acquisition card (NI 9239, National Instruments) and the data was recorded on a PC running LabVIEW 8.5 (National Instruments). When measuring the solids mass flow rate, the valve *(12)* on the return line *(13)* was fully closed. At the end of an experimental run, the valve on the return line was opened to discharge the collected material back to the feed tank.

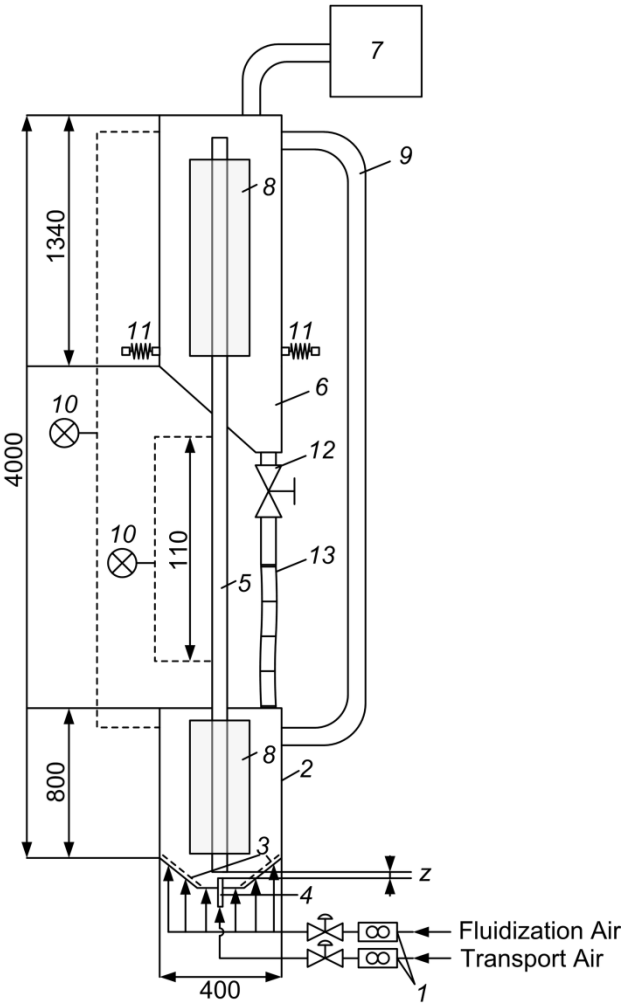

Figure 1 Schematic diagram of the vertical air-lift: 1-flowmeters, 2-feed tank, 3-air distribution plate, 4-nozzle, 5-transport pipe, 6-receiving tank, 7-bag filter, 8-inspection glass, 9-bleed line, 10-differential pressure transmitters, 11-load cells, 12-butterfly valve, and 13-return line.

2.2. Operating conditions

The transport air flow rate and the fluidization air flow rate were varied during the experiments in order to study their effects on the solids mass flow rate and the pipeline pressure drop. The transport air flow rate ranged from 24 to 100 Nm^3/h. This corresponds to the superficial air velocity of about 5 to 21 m/s, respectively, assuming that all the air passing through the nozzle enters the transport pipe. The fluidization air flow rate was varied between 0–12 Nm^3/h for glass beads and 0–60 Nm^3/h for zirconium oxide. Figure 2 shows a typical micrograph of the particles taken by an Olympus BH2 optical microscope equipped with a Moticam 2300 high-resolution digital camera.

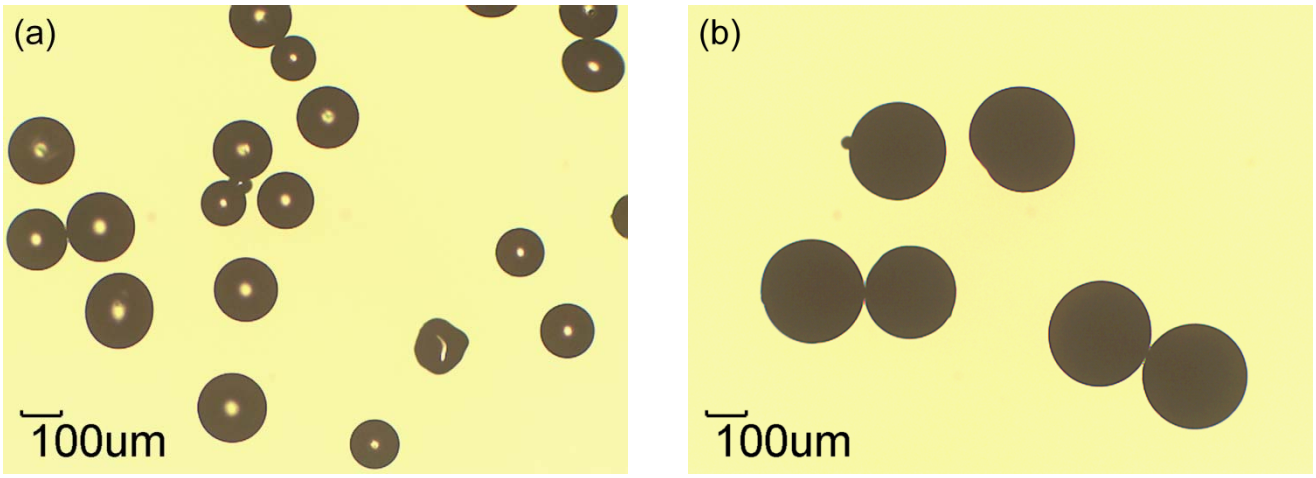

Figure 2 Particle micrographs, (a) glass beads ad (b) zirconium oxide.

The micrographs revealed that the particles of both materials were fairly spherical. Other properties of the particles are summarized in Table 1.

Table 1 Material properties.

Material	Particle size (μm)	Average particle diameter (μm) [a]	Particle density (kg/m^3)	U_t (m/s) [b]	U_{mf} (m/s) [c]
Glass beads	100–200	150	2500	0.9	0.019
Zirconium oxide	200–300	260	3800	2.3	0.102

[a] Determined by sieving analysis.
[b] Ut is the particle terminal velocity.
[c] Umf is the minimum fluidization velocity.

The particle terminal velocity (U_t) was calculated based on the correlation given by Klinzing *et al.* [1] for intermediate regime (Re_{pf} = 0.5–500). The minimum fluidization velocity (U_{mf}) was measured with a fluidization tester (built at Dept. POSTEC, Tel-Tek, Norway). Although U_{mf} for glass and zirconium oxide particles differs by factor of 5, both materials classify as group B (sand-like) particles according

to the Geldart's classification [15]. Materials in Group B are characterized by formation of bubbles and a small bed expansion at the onset of fluidization. Due to their poor air retention capability, the fluidized bed tends to collapse quickly when the gas supply is suddenly turned off [15].

2.3. Measurement of solids mass flow rate and pressure drop

Unlike in industrial systems, the vertical air-lift illustrated in Figure 1 was operated in a discontinuous mode. The material was filled into the feed tank prior to conducting the tests. To measure the solids mass flow rate, the valve on the return line (*12* in Figure 1) was closed and the conveyed solids were collected in the receiving tank. After the measurement, the valve on the return line was opened to discharge the material back to the feed tank. In such a set-up, the level of the solids bed (i.e., the hydrostatic pressure) in the feed tank gradually decreased during the pneumatic transport. As a consequence, the solids mass flow rate (solids mass per unit time) and the pressure drop in the transport pipe also decreased (Figure 3).

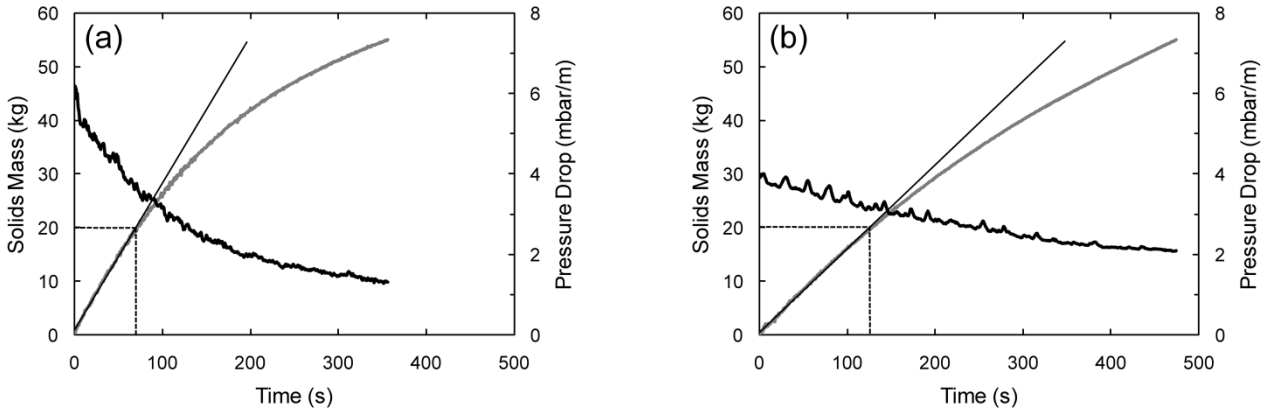

Figure 3 Solids mass (grey) and pressure drop (black) as a function of time during pneumatic transport of glass beads (a) and zirconium oxide (b). Operating conditions: transport air flow rate 69 Nm^3/h, fluidization air flow rate 12 Nm^3/h.

To eliminate the effect of hydrostatic pressure, the pressure drop was measured with the valve on the return line fully open. Thus, the solids circulated between the feed and the receiving tank and the level of the solids bed in the feed tank remained constant during the measurement. Due to fluctuations in pressure drop (especially at low transport air velocities), the data was collected over a period of 5 min and the values were averaged. The degree of pressure fluctuations was quantified in terms of standard deviation. After the pressure drop has been measured, the valve on the return line was closed and the rate of the solids accumulation in the receiving tank was measured. The solids mass flow rate was calculated from the initial slope of the solids accumulation curve up to 20 kg for each experiment (Figure 3). To maintain a consistent hydrostatic pressure in all experiments, the total mass of the solids

in the feed tank was about 60 kg for both glass and zirconium oxide particles. Due to the difference in particle size and density, the height of the solids bed was 42 cm and 33 cm for glass and zirconium oxide particles, respectively, measured from the bottom of the feed tank.

3. Results and Discussion

3.1. Solids mass flow rate

In vertical air-lifts with a fluidized bed feeding system, the solids mass flow rate cannot be controlled independently but it is a function of the fluidization air flow rate, transport air flow rate, nozzle position (distance *z*), height of the fluidized bed, and length and diameter of the transport pipe [5-7]. In our experiments, only the fluidization and transport air flow rates were varied while the rest of the factors remained constant. The solids mass flow rate is plotted as a function of the fluidization air flow rate for different transport air velocities in Figure 4 for glass beads (a) and zirconium oxide (b).

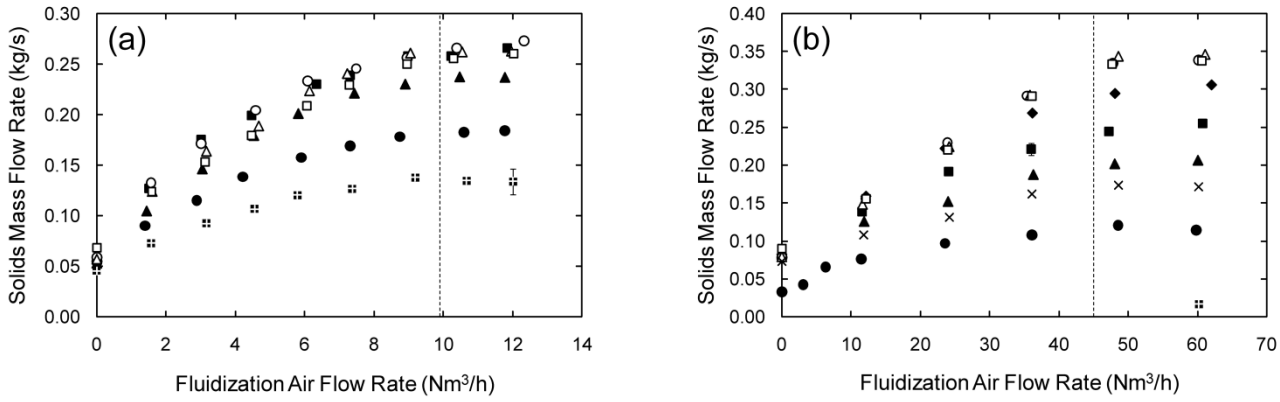

Figure 4 Solids mass flow rate as a function of fluidization air flow rate for different transport air velocities, (a) glass beads and (b) zirconium oxide: (▪) 5.2 m/s, (●) 6.9 m/s, (×) 8.0 m/s, (▲) 8.7 m/s, (■) 10.4 m/s, (◆) 12.1 m/s, (○) 13.9 m/s, (△) 17.3 m/s, and (□) 20.8 m/s. Error bars represent standard deviation (n=2). The dotted line represents onset of fluidization.

The solids mass flow rate increases with increasing fluidization air flow rate up to approximately 10 Nm^3/h for glass beads and 48 Nm^3/h for zirconium oxide and then levels off. Visual observation of the solids bed through the glass window in the feed tank revealed that fluidization began around 9.9 Nm^3/h for glass beads and 45.0 Nm^3/h for zirconium oxide (marked by the dotted line in Figure 4). Taking into account the diameter of the feed tank (0.4 m), this corresponds to the superficial fluidization velocity of 0.022 and 0.100 m/s for glass beads and zirconium oxide, respectively, which is in agreement with the measured minimum fluidization velocities (Table 1). The fluidization air flow rate thus increases the solids mass flow rate only until the solids bed becomes fully fluidized. It is apparent that at least for Geldart's B particles, further increase in fluidization air flow rate above the fluidization point has no

effect on the solids mass flow rate. For this reason, pneumatic conveyors with a fluidized bed solids feeder such as vertical air-lift should be operated at or slightly above the minimum fluidization velocity [6].

To demonstrate the effect of the transport air velocity on the solids mass flow rate, the data in Figure 4 was replotted in Figure 5.

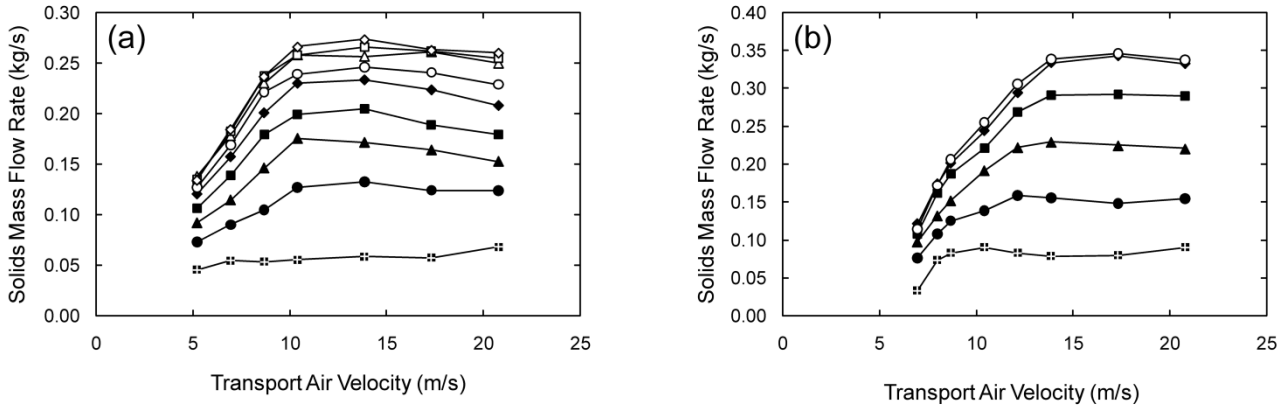

Figure 5 Solids mass flow rate as a function of transport air velocity for different fluidization air flow rates, (a) glass beads: (▪) 0.0 Nm^3/h, (●) 1.5 Nm^3/h, (▲) 3.0 Nm^3/h, (■) 4.5 Nm^3/h, (◆) 6.0 Nm^3/h, (○) 7.5 Nm^3/h, (△) 9.0 Nm^3/h, (□) 10.5 Nm^3/h, (◇) 12.0 Nm^3/h and (b) zirconium oxide: (▪) 0 Nm^3/h, (●) 12.0 Nm^3/h, (▲) 24.0 Nm^3/h, (■) 36.0 Nm^3/h, (◆) 48.0 Nm^3/h, (○) 60.0 Nm^3/h.

Apart from the fluidization air flow rate of 0 Nm^3/h, both materials display the same qualitative behavior. The solids mass flow rate initially increases with increasing transport air velocity up to 10 m/s for glass beads and 14 m/s for zirconium oxide. At higher transport air velocities, it becomes unclear whether the solids mass flow rate slightly decreases or reaches a plateau. Similar trends were reported by others [5, 9] for vertical pneumatic conveyors equipped with a fluidized/spouted bed feeding device. Decamps *et al.* [5] reported that the solids mass flow rate increased with increasing transport air velocity, reached a maximum, and further decreased. The decrease in solids mass flow rate at higher transport air velocities was explained by reduced tube filling. Indeed, the solids loading ratio (solids to gas mass flow rate ratio) decreases at transport air velocities higher than 14 m/s for both glass beads and zirconium oxide (Figure 6). However, it can be expected that at the same time, the particle velocity increases with increasing transport air velocity [7, 8], which could explain why in our study, the solids mass flow rate remains more or less constant at higher transport air velocities (Figure 5).

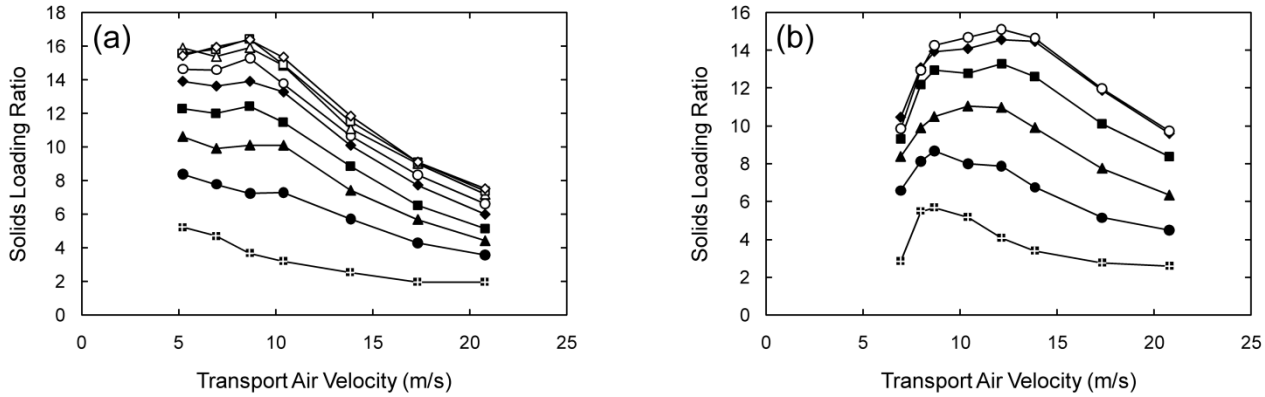

Figure 6 Solids loading ratio as a function of transport air velocity for different fluidization air flow rates, (a) glass beads and (b) zirconium oxide. For symbol legend, see Figure 5.

3.2. Pressure Drop

To characterize the flow behavior in pneumatic conveying of glass and zirconium oxide particles in the vertical air-lift, pressure gradient along the transport pipe was measured simultaneously with the solids mass flow rate in all experiments. As shown in Figure 7, the pressure drop followed the same qualitative behavior as the solids mass flow rate when plotted as a function of the fluidization air flow rate. After the solids bed becomes fully fluidized (marked by the dotted line in Figure 7), the pressure drop seems leveling off with further increase in fluidization air flow rate. It is also apparent that at lower fluidization air flow rates (0–6 Nm^3/h), the curve corresponding to the lowest transport air velocity (6.9 m/s) in Figure 7 (b) deviates from the general behavior.

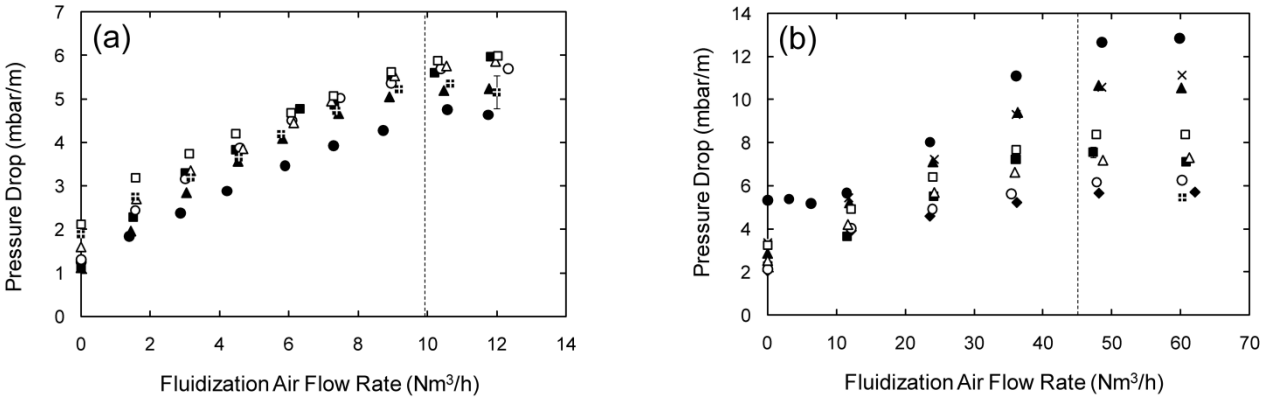

Figure 7 Pressure drop as a function of fluidization air flow rate for different transport air velocities, (a) glass beads and (b) zirconium oxide. For symbol legend, see Figure 4. Error bars represent standard deviation (n=2). The dotted line represents onset of fluidization.

Although the solids mass flow rate corresponding to the same operating conditions was less than 0.07 kg/s (Figure 4 (b)), the measured pressure drop was surprisingly high (5.4 mbar/m) and exhibited significant fluctuations during the 5 minute-long measurement period (as will be shown later). The transport air velocity of 6.9 m/s is only three times higher than the terminal velocity of the zirconium oxide particles (Table 1), which may not be high enough to maintain the solids in suspension and to keep them moving upward. Consequently, the solids mass flow rate becomes low while the pressure drop remains high due to instabilities in the gas-solid flow. Decreasing the transport air velocity to 5.2 m/s while keeping the solids bed in the feed tank fully fluidized resulted in poor solids mass flow rate (Figure 4 (b)) but the average pressure drop remained at 5.4 mbar/m (Figure 7 (b)). Similar behavior was not observed for glass beads, which are smaller and lighter than the zirconium oxide particles. The ratio between the lowest tested transport air velocity (5.2 m/s) and the terminal velocity was more than twice as high for glass compared with zirconium oxide.

3.3. Solids mass flow rate versus pressure drop

The data obtained from the measurements of the pipeline pressure drop and the solids mass flow rate in the vertical air-lift was plotted in Figure 8 for different transport air velocities. Since the solids mass flow rate could not be set independently, different levels of the solids mass flow rate had to be obtained by varying the fluidization air flow rate. Keeping the transport air velocity constant, the minimum solids mass flow rate was achieved at zero fluidization air flow rate while the maximum was reached when the solids bed in the feed tank became fully fluidized (Figure 4). Every curve in Figure 8 thus represents measurements obtained at constant transport air velocity and fluidization air flow rate ranging between 0–9 Nm^3/h for glass and 0–48 Nm^3/h for zirconium oxide. The pressure drop values at zero solids mass flow rate correspond to the pressure drop measured for air flow only. The pressure drop for zirconium oxide was generally higher than that for glass beads when compared at similar conditions, which can be explained by higher drag forces associated with the transport of larger and heavier solid particles. The difference in pressure drop between the two materials was especially pronounced at lower transport air velocities and diminished as the transport air velocity increased (Figure 8 (c)). The data points obtained at the lowest transport air velocity for glass beads (Figure 8 (a)) could be represented by a linear function. However, at higher transport air velocities (6.9–20.8 m/s), the pressure drop clearly increased with the solids mass flow rate at an increasing rate. Similar trend between the pressure drop and the solids mass flow rate was also observed for zirconium oxide (Figure 8 (b)) but only at transport air velocities in the range of 8.0 to 10.4 m/s. At higher transport air velocities, the pressure drop continued increasing with the solids mass flow rate but at a decreasing rate.

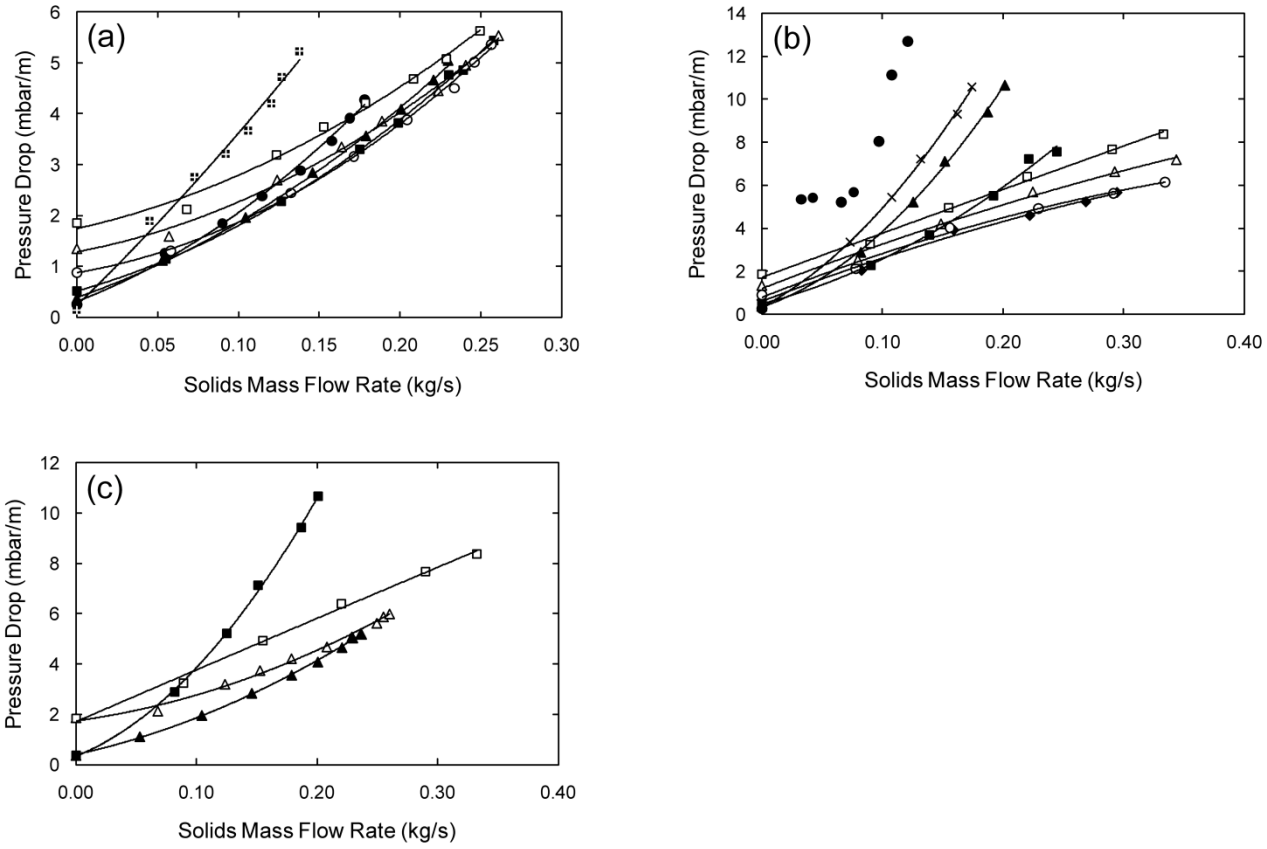

Figure 8 Pressure drop as a function of solids mass flow rate for different transport air velocities, (a) glass beads and (b) zirconium oxide (for symbol legend of (a) and (b), see Figure 4), (c) comparison between glass (triangles) and zirconium oxide (squares) at the transport air velocity of 8.7 m/s (closed symbols) and 20.8 m/s (open symbols). Solid lines represent the best fit based on quadratic equation.

The solid lines in Figure 8 represent the best fit based on quadratic equation ($y = Ax^2 + Bx + C$) with R^2 values higher than 0.99. The numerical values of A, B, C coefficients are presented in Table 2. Note that the data set corresponding to the lowest transport air velocity (6.9 m/s) in Figure 8 (b) was excluded from the curve fitting analysis.

Table 2 Numerical values of coefficients A, B, C obtained from the best fit curves in Figure 8 based on quadratic equation ($y = Ax^2 + Bx + C$).

Transport air velocity (m/s)	Glass beads			Zirconium oxide		
	A	B	C	A	B	C
5.2	30.1	30.9	0.2	-	-	-
6.9	54.9	12.0	0.3	-	-	-
8.0	-	-	-	166.5	29.5	0.3
8.7	39.1	10.9	0.4	159.9	19.1	0.3
10.4	39.8	8.9	0.5	63.3	14.6	0.5
12.1	-	-	-	-15.8	21.7	0.6
13.9	46.7	5.3	0.9	-18.7	22.3	0.8
17.3	39.2	5.9	1.3	-12.0	21.9	1.2
20.8	34.4	7.1	1.7	-0.8	20.6	1.7

The relationship between the transport air velocity, the solids mass flow rate, and the pressure drop is commonly presented in the literature in the form of state diagrams where the pressure drop is plotted as a function of transport air velocity for different solids mass flow rates. It is generally accepted that the pressure drop increases with higher solids mass flow rate but the quantitative relationship cannot be readily inferred from the state diagrams. In a few literature studies, where the pressure drop was plotted as a function of solids mass flow rate or suspension density (mass of solids transported per unit volume of air), a linear dependence was observed over a wide range of transport air velocities [12, 14, 16-18]. The knowledge of the relationship between the solids mass flow rate and the pressure drop would be extremely beneficial, as it would allow direct prediction of one from the other, thus saving expenses for costly measuring equipment. Our study suggests, that at least for the vertical air-lift, the pressure drop is non-linearly related to the solids mass flow rate.

The total pressure drop (ΔP) in the fully developed region in vertical pneumatic conveying is composed of gravitational and frictional pressure loss. The former arises from the static contributions of the gas-solid mixture (ΔP_{gg} and ΔP_{gs}) while the latter accounts for the gas-wall (ΔP_{fg}) and the solids-wall friction (ΔP_{fs}). The total pressure drop can be then expressed as follows:

$$\frac{\Delta P}{\Delta L} = \frac{1}{\Delta L}(\Delta P_{gg} + \Delta P_{gs} + \Delta P_{fg} + \Delta P_{fs}) = \rho_g \varepsilon g + \rho_s (1-\varepsilon) g + \frac{\lambda_g \rho_g U_g^2}{2D} + \frac{\lambda_{fs} \rho_s (1-\varepsilon) U_s^2}{2D} \quad (1)$$

where ΔL is the pipe length, ρ_g is the gas density, ε is the bed voidage, g is the gravitational acceleration, ρ_s is the density of the solid particles, λ_g is the gas friction factor, U_g is the transport air velocity, D is the pipe diameter, λ_{fs} is the solids impact and friction factor, and U_s is the solids velocity. The static contribution due to gas alone (ΔP_{gg}) is usually ignored, because it is negligible in comparison with the other terms in Eq. (1). According to Klinzing *et al.* [1], the solids gravitational and frictional contribution (i.e., the overall solids contribution to the pressure drop, ΔP_s) is equivalent to:

$$\frac{\Delta P_s}{\Delta L} = \frac{1}{\Delta L}(\Delta P_{gs} + \Delta P_{fs}) = \rho_s (1 - \varepsilon) g + \frac{\lambda_{fs} \rho_s (1 - \varepsilon) U_s^2}{2D} = \frac{\mu \lambda_s \rho_g U_g^2}{2D} \quad (2)$$

where μ is the solids loading ratio and λ_s is the additional pressure drop coefficient due to the presence of solids in the gas flow. Since the gas frictional pressure drop is typically considered constant at constant transport air velocity, the total pressure drop (ΔP) is mainly governed by the overall solids contribution (ΔP_s). From Eq. (2), it then becomes apparent that the total pressure drop should be directly proportional to the solids mass loading at constant transport air velocity, which is in line with the results reported in the literature [12, 14, 16-18]. However, considering that the solids velocity can be expressed

as a function of the solids mass flow rate (G_s), the density of the solid particles (ρ_s) and the solids concentration ($1-\varepsilon$),

$$U_s = \frac{G_s}{\rho_s(1-\varepsilon)} \tag{3}$$

and substituting Eq. (3) into Eq. (1), the relationship between the solids mass flow rate and the pressure drop becomes less obvious.

It is believed that the pressure drop dependence on the solids mass flow rate observed in our study (Figure 8) is a result of an interplay between the solids gravitational (ΔP_{gs}) and frictional (ΔP_{fs}) pressure drop components, which is affected by the particle properties. At low transport air velocities, the solids concentration ($1-\varepsilon$) is high and increases at a faster rate with the solids mass flow rate than at higher transport air velocities [19]. As a result, the pressure drop rises faster with the solids mass flow rate at lower transport air velocities. The high pressure drop observed at the lowest transport air velocity (5.2 m/s for glass and 6.9 m/s for zirconium oxide) is predominantly caused by the gravitational pressure drop component, which is more significant for zirconium oxide than for glass beads. As the transport air velocity increases, the gravitational pressure drop becomes less important and the frictional component starts increasing. The equilibrium between the gravitational and the frictional pressure drop is achieved at a lower transport air velocity for glass beads than for zirconium oxide. A clear transition from a convex to concave curvature of the pressure drop versus the solids mass flow rate relationship at the transport air velocity between 10.4 and 12.1 m/s marks this equilibrium point for the zirconium oxide particles. This is also reflected by the change of sign of the coefficient A in Table 2.

Costa *et al.* [20] investigated the effect of particle diameter on voidage (ε) in vertical pneumatic conveying of glass spheres (1.00, 1.70, and 2.85 mm) using different solids feeding systems (spouted bed feeder, screw feeder, and gravitational feeder). The voidage decreased with decreasing transport air velocity and increasing particle diameter for all solids feeding systems but the dependence was more significant for the spouted bed feeder compared with the other feeding devices. The effect of particle diameter on voidage was especially pronounced at low transport air velocities and decreased as the transport air velocity increased. These observations could explain the large difference between the pressure drop values for glass beads and zirconium oxide at low transport air velocities in our study. As the transport air velocity increases, the voidage becomes less dependent on the transport air velocity and the particle diameter and the difference in pressure drop between glass beads and zirconium oxide decreases. Since the voidage decreases faster with decreasing transport air velocity for larger particles [20], the gravitational pressure drop would exceed the frictional pressure drop at a higher transport air velocity for zirconium oxide than for glass beads. However, further measurements of voidage, solids

velocity, and solids friction factor are required to verify this hypothesis and clarify the effects of particle properties on the pressure drop.

3.4. State diagrams

In most of the pneumatic conveying systems, the solids and the gas flow rate can be independently set, which allows straightforward design of experiments and construction of state diagrams. In vertical air-lifts, however, construction of state diagrams is more challenging, because the solids mass flow rate is dependent on the fluidization air flow rate. Therefore, the state diagrams in Figure 9 had to be derived from the best fit quadratic equations presented in Figure 8 with the coefficients A, B, C reported in Table 2. To avoid extrapolation to higher solids mass flow rates (especially at low transport air velocities), the pressure drop was calculated only for the solids mass flow rates up to 0.125 kg/s for both glass and zirconium oxide. The pressure drop profiles display a typical trend. As the transport air velocity decreases at constant solids mass flow rate, the pressure drop decreases, goes through a minimum, and increases. This indicates the presence of both dense and dilute phase regimes in pneumatic conveying of glass and zirconium oxide particles under given experimental conditions. The pressure gradients are clearly higher for the larger and heavier zirconium oxide particles and shifted to the right with respect to the glass bead system. The pressure drop curves for glass beads display relatively shallow minima in comparison with those for zirconium oxide.

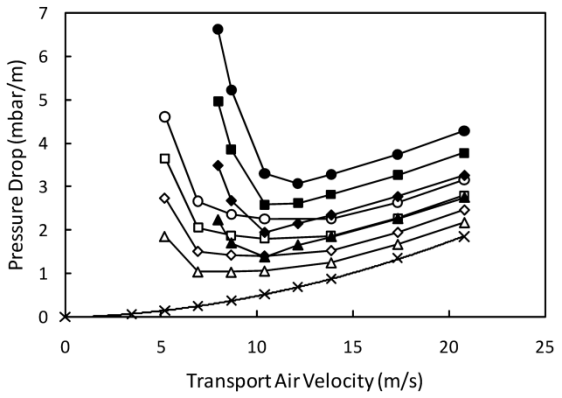

Figure 9 State diagrams illustrating the pressure drop as a function of transport air velocity for different solids mass flow rate: 0.050 kg/s (triangles), 0.075 kg/s (diamonds), 0.100 kg/s (squares), and 0.125 kg/s (circles) for glass beads (open symbols) and zirconium oxide (closed symbols).

To find the exact location of the minimum pressure drop on each curve is rather difficult, nonetheless, it is apparent that when the solids mass flow rate is increased, the minimum pressure drop increases with increasing transport air velocity faster for zirconium oxide than it does for glass beads. One can assume that for the solids mass flow rates tested, the minimum pressure drop lies approximately in the velocity

range of 7 to 10 m/s for glass beads and 10 to 12 m/s for zirconium oxide. The shift of the pressure drop minimum towards higher transport air velocities for the zirconium oxide particles is expected, because the energy required for the transport increases with increasing particle size and density [11, 14]. Since both materials differ in particle size and density, it is not possible to clearly set apart the individual effects of both parameters on the pressure gradients. Further experiments should be conducted to estimate individual contributions of particle size and density on the pressure gradient profiles.

3.5. Pressure drop fluctuations

Analysis of the pressure fluctuations has been used as a tool for identifying the flow regime in both horizontal and vertical pneumatic conveying [20-22]. Costa *et al.* [20] and Grbavcic *et al.* [22] used standard deviation of local fluid static pressure plotted as a function of gas superficial velocity to determine the transition between dilute phase and slug flow regime in vertical pneumatic conveying of coarse particles. In both studies, the transitional points were recognized from the change in slope of a linear relationship between the standard deviation of pressure drop and the transport air velocity. Similarly, we have used standard deviation to quantify the degree of pressure drop fluctuations measured during pneumatic conveying of glass and zirconium oxide particles under numerous experimental conditions. As mentioned above (Section 2.3), the pressure drop data was collected over a period of 5 min for each experiment and the values were averaged. Standard deviation calculated from the recorded data thus represents the variability of the pressure drop signal.

Since the solids mass flow rate could not be fixed at a particular value (due to the use of the fluidized bed feeder), we decided to plot the standard deviation rather as a function of the solids mass flow rate for different transport air velocities. The data in Figure 10 indicate that the standard deviation increases with increasing solids mass flow rate for both materials, which can be attributed to higher degree of particle-wall and particle-particle collisions. For a given solids mass flow rate, the pressure drop fluctuations are strongest at the lowest transport air velocity and tend to decrease with increasing transport air velocity. Such a trend is overall consistent with the published data [20, 22]. One also infers that the standard deviation at low transport air velocity is almost twice as high for zirconium oxide when compared with glass beads. However, since the average pressure drop was also higher for zirconium oxide (Figure 7), the relative standard deviation (i.e., standard deviation divided by average $\times$ 100 %) turns out to be comparable for both types of particles. The pressure drop fluctuations become significantly reduced at transport air velocities above 8.7 m/s for glass beads and above 12.1 m/s for zirconium oxide. These values are in rough agreement with the range of the minimum pressure drop velocities visually estimated from the state diagrams in Figure 9. From the analysis above, one concludes that statistical parameters of the pressure drop fluctuations can be successfully used to

determine the transition between dense and dilute phase conveying also in vertical air-lifts, which could be of great importance for industrial practice.

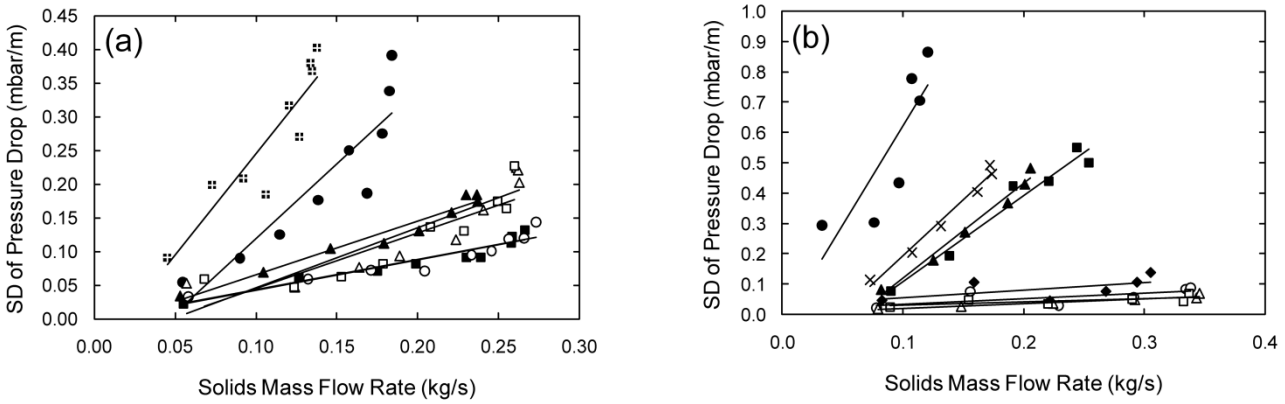

Figure 10 Standard deviation (SD) of the pressure drop signal as a function of solids mass flow rate for different transport air velocities, (a) glass beads and (b) zirconium oxide. For symbol legend, see Figure 4.

4. Conclusion

The presented study investigates the effect of the fluidization air flow rate and the transport air velocity on the solids mass flow rate and the pipeline pressure drop in pneumatic conveying of Geldart's B particles in the vertical air-lift. The pneumatic conveying characteristics are compared for two materials, glass beads with average particle diameter of 150 μm and particle density of 2500 kg/m^3 and zirconium oxide with average particle diameter of 260 μm and particle density of 3800 kg/m^3. For a given transport air velocity, the solids mass flow rate and the pipeline pressure drop increased with increasing fluidization air flow rate until the solids bed in the feed tank became fully fluidized. At constant fluidization air flow rate, the solids mass flow rate first increased with increasing transport air velocity until a plateau was reached. The pipeline pressure drop was a function of the solids mass flow rate but the quantitative relationship was dependent on the transport air velocity and the type of material. The pressure drop for zirconium oxide was always higher than that for glass beads at similar conditions but the difference was more accentuated at lower transport air velocities. This was attributed to the contribution of the gravitational pressure drop, which is expected to be more significant for the zirconium oxide particles due to their larger particle diameter and higher density. The presence of both dense and dilute phase regime was indicated by the state diagrams for both materials under given experimental conditions. The minimum pressure drop was higher for the larger and heavier zirconium oxide particles and was reached at higher transport air velocities when compared with glass beads. The transition from dense to dilute phase regime was also apparent from the analysis of the standard deviation of the pressure drop fluctuations at different transport air velocities.

This study provides important information about the relationship between the transport air velocity, the solids mass flow rate, and the pipeline pressure drop during pneumatic conveying in vertical air-lifts. One interesting observation is that the quantitative relationship between the solids mass flow rate and the pipeline pressure drop is dependent on the transport air velocity and the type of conveyed material, a finding that should be further explored. Our results suggest that the analysis of the pressure drop fluctuations can be useful in identifying the flow regime and selecting a suitable gas working velocity. Future work will investigate the effects of particle size and density on pressure drop for materials from different groups of the Geldart's classification. Special focus will be given to the measurements of voidage, solids velocity, and solids friction factor to clarify the effect of the solids mass flow rate on the pressure drop for solids with different particle properties.

Nomenclature

D	pipe diameter (m)
g	gravitational acceleration (m/s^2)
G_s	solids mass flow rate ($kg/(m^2 \cdot s)$)
ΔL	pipe length (m)
ΔP	total pressure drop (Pa)
ΔP_{fg}	pressure drop due to gas-wall friction (Pa)
ΔP_{fs}	pressure drop due to solids-wall friction (Pa)
ΔP_{gg}	gravitational pressure drop due to gas (Pa)
ΔP_{gs}	gravitational pressure drop due to solids (Pa)
ΔP_s	overall pressure drop due to presence of solids (Pa)
Re_{pf}	Reynolds number related to terminal velocity of a particle (-)
U_g	superficial transport air velocity (m/s)
U_{mf}	minimum fluidization velocity (m/s)
U_s	solids velocity (m/s)
U_t	terminal velocity of a particle (m/s)
ε	bed voidage (-)
λ_g	gas friction factor (-)
λ_{fs}	solids impact and friction factor (-)
λ_s	additional pressure drop coefficient due to presence of solids (-)
μ	solids loading ratio (-)
ρ_g	gas density (kg/m^3)
ρ_s	density of solid particles (kg/m^3)

Acknowledgement

This work has been part of the strategic research program, Experimental and simulation studies of gas-particulate flow systems (GASPARFLO). The financial support by the Research Council of Norway is gratefully acknowledged.

REFERENCES

[1] Klinzing GE, Marcus RD, Rizk F, Leung LS. Pneumatic conveying of solids: A theoretical and practical approach. London: Chapman & Hall 1997.

[2] Kraus MN. Pneumatic conveying of bulk materials. 2nd ed. New York: McGraw-Hill Publications Co. 1980.

[3] Molerus O. Overview: Pneumatic transport of solids. Powder Technology. 1996;88(3):309-21.

[4] Stoess HA, Jr. Pneumatic conveying. New York: Wiley-Interscience 1970.

[5] Decamps F, Dumont G, Goossens W. Vertical pneumatic conveyor with a fluidized bed as mixing zone. Powder Technology. 1972;5(5):299-306.

[6] Leung LS, Towler BF. Design of vertical pneumatic conveyor with a fluidized bed as mixing zone. Powder Technology. 1973;8(1-2):27-32.

[7] Mathiesen V, Solberg T. Laser-based flow measurements of dilute vertical pneumatic transport. Chem Eng Commun. 2004;191(3).

[8] Mathisen A, Halvorsen B, Melaaen MC. Experimental study of dilute vertical pneumatic transport using PIV. RELPOWFLO IV. Tromsø, Norway: Telemark Technological Research and Development Centre 2008:569-75.

[9] Garic RV, Grbavcic ZB, Jovanovic SD. Hydrodynamic modeling of vertical non-accelerating gas-solids flow. Powder Technology. 1995;84(1):65-74.

[10] Raczek J, Palica M. Selection of the gas working velocity in vertical pneumatic conveying systems for binary mixtures. Chem Eng Process. 1997;36(2):167-70.

[11] Narimatsu CP, Ferreira MC. Vertical pneumatic conveying in dilute and dense-phase flows: Experimental study of the influence of particle density and diameter on fluid dynamic behavior. Braz J Chem Eng. 2001;18:221-32.

[12] Wang FJ, Zhu JX, Beeckmans JM. Pressure gradient and particle adhesion in the pneumatic transport of cohesive fine powders. Int J Multiphase Flow. 2000;26(2):245-65.

[13] Herbreteau C, Bouard R. Experimental study of parameters which influence the energy minimum in horizontal gas–solid conveying. Powder Technology. 2000;112:213-20.

[14] Hyder LM, Bradley MSA, Reed AR, Hettiaratchi K. An investigation into the effect of particle size on straight-pipe pressure gradients in lean-phase conveying. Powder Technology. 2000;112(3):235-43.

[15] Geldart D. Types of gas fluidization. Powder Technology. 1973;7:285-92.

[16] Jotaki T, Tomita Y, Fujimoto K, Iwasaki M. Pressure drop in an equilibrium region of vertical pneumatic transport of granular solids. Bulletin of JSME. 1978 19780100;21(151):128-33.

[17] Hettiaratchi K, Woodhead SR, Reed AR. Comparison between pressure drop in horizontal and vertical pneumatic conveying pipelines. Powder Technology. 1998;95(1):67-73.

[18] Hettiaratchi K, Bradley MSA, Farnish RJ, Bridle I, Hyder LM, Reed AR. An investigation into the effect of product type when scaling for diameter in vertical pipelines. Powder Technology. 2000;112(3):229-34.

[19] Rautiainen A, Stewart G, Poikolainen V, Sarkomaa P. An experimental study of vertical pneumatic conveying. Powder Technology. 1999;104(2):139-50.

[20] Costa IA, Ferreira MC, Freire JT. Analysis of regime transitions and flow instabilities in vertical conveying of coarse particles using different solids feeding systems. Can J Chem Eng. 2004;82(1):48-59.

[21] Jama GA, Klinzing GE, Rizk F. An investigation of the prevailing flow patterns and pressure fluctuation near the pressure minimum and unstable conveying zone of pneumatic transport systems. Powder Technology. 2000;112:87-93.

[22] Grbavcic ZB, Garic-Grulovic RV, Arsenijevic ZL. Prediction of the choking velocity and voidage in vertical pneumatic conveying of coarse particles. Powder Technology. 2006;161(1):1-9.